

Hybrid magnetic graphitic nanocomposites for catalytic wet peroxide oxidation applications

Rui S. Ribeiro^a, Adrián M.T. Silva^b, Pedro B. Tavares^c, José L. Figueiredo^b,
Joaquim L. Faria^b, Helder T. Gomes^{a,*}

^a *Laboratory of Separation and Reaction Engineering - Laboratory of Catalysis and Materials (LSRE-LCM), Departamento de Tecnologia Química e Biológica, Escola Superior de Tecnologia e Gestão, Instituto Politécnico de Bragança, Campus de Santa Apolónia, 5300-253 Bragança, Portugal.*

^b *Laboratory of Separation and Reaction Engineering - Laboratory of Catalysis and Materials (LSRE-LCM), Faculdade de Engenharia, Universidade do Porto, Rua Dr. Roberto Frias, 4200-465 Porto, Portugal.*

^c *CQVR – Centro de Química - Vila Real, Universidade de Trás-os-Montes e Alto Douro, 5000-801 Vila Real, Portugal.*

*Corresponding author.

Tel.: +351 273 303 110; Fax: +351 273 313 051; E-mail address: htgomes@ipb.pt

This article has been accepted for publication and undergone full peer review.
Please cite this article as DOI: 10.1016/j.cattod.2016.04.040

Abstract

Fe_3O_4 , with a lattice parameter $a = 8.357 \text{ \AA}$ and average particle size of $12.5 \pm 3.6 \text{ nm}$, was successfully encapsulated within a graphitic structure by a hierarchical co-assembly approach, followed by thermal annealing. The resulting material was denoted as MGNC – magnetic graphitic nanocomposite. MGNC possesses average core size of $109 \pm 35 \text{ nm}$ (mainly composed by agglomerates of magnetic nanoparticles), stability up to $400 \text{ }^\circ\text{C}$ under oxidizing atmosphere, a micro-mesoporous structure with a fairly developed specific surface area ($S_{\text{BET}} = 330 \text{ m}^2 \text{ g}^{-1}$) and neutral character ($\text{pH}_{\text{PZC}} = 7.1$).

Catalytic wet peroxide oxidation (CWPO) experiments performed with a 4-nitrophenol (4-NP)/ Fe_3O_4 mass ratio fixed at 36.6, allowed to achieve high efficiency of catalyst usage throughout the wide range of 4-NP concentration considered ($200 \text{ mg L}^{-1} - 5 \text{ g L}^{-1}$). The inclusion of Fe_3O_4 nanoparticles in a graphitic structure during the synthesis of MGNC was found to (i) enhance the catalytic activity in CWPO when compared to Fe_3O_4 , due to increased adsorptive interactions between the surface of the catalyst and the pollutant molecules, while (ii) strongly limiting the leaching of Fe species from Fe_3O_4 to the treated water, due to the confinement effect caused by the carbon shell.

As a result of these effects, unprecedented pollutant mass removals were obtained – ranging from $5000 \text{ mg g}^{-1} \text{ h}^{-1}$, when the CWPO process is performed with $[\text{4-NP}]_0 = 200 \text{ mg L}^{-1}$ at $\text{pH} = 3$, to $1250 \text{ mg g}^{-1} \text{ h}^{-1}$, when $[\text{4-NP}]_0 = 5 \text{ g L}^{-1}$. High efficiency of H_2O_2 consumption is obtained when MGNC is applied in the CWPO of 4-NP solutions at $\text{pH} = 3$, with TOC removals per unit of H_2O_2 decomposed ($\eta_{\text{H}_2\text{O}_2}$) in the range 64 – 100%. In addition, the MGNC catalyst is also active at $\text{pH} = 6$; in this case a pollutant mass removal of $2090 \text{ mg g}^{-1} \text{ h}^{-1}$ was obtained.

Although MGNC partially deactivates through successive reusability cycles, the pollutant mass removal obtained at the end of the fourth cycle is still very high when 200

mg L⁻¹ 4-NP solutions are considered (4808 mg g⁻¹ h⁻¹, representing only a ca. 4% decrease when compared to the first cycle). A higher deactivation of the MGNC catalyst is observed when 5 g L⁻¹ 4-NP solutions are employed. Nevertheless, the pollutant mass removal obtained at the end of the third cycle is still high (551 mg g⁻¹ h⁻¹).

Keywords: Magnetic nanoparticles (MNP); Core-shell nanocomposites; Catalytic wet peroxide oxidation (CWPO); Heterogeneous Fenton process.

1. Introduction

The development of efficient and economically viable treatment technologies, able to cope with the increasing complexity of industrial wastewaters, is an ongoing challenge for the scientific community. In particular, toxic and refractory compounds like phenols and nitrophenols – often found in industrial wastewaters, such as those from pharmaceutical, petrochemical, metallurgical, textile, rubber and plastic industries, refineries, fungicides and even from municipal landfill leachates [1-6] – can have a negative impact on conventional biological wastewater treatment processes. Therefore, other treatment options should be considered. In this context, the so-called advanced oxidation processes (AOP) are usually seen as a powerful tool [7], since they rely on the formation of highly oxidizing hydroxyl radicals, HO• (standard reduction potential between +2.8 V and +2.0 V at pH 0 and 14, respectively), which serve as effective species for the destruction of a huge range of refractory organic pollutants [8, 9].

Catalytic wet peroxide oxidation (CWPO) is an AOP characterized by the formation of HO• radicals from the catalytic decomposition of hydrogen peroxide (H₂O₂) performed at low temperature and atmospheric pressure [10, 11]. Therefore, CWPO is widely recognized as a low cost AOP [11, 12]. However, as recently reviewed, further optimization of catalyst design is still required in order to bring CWPO to the forefront of the most efficient AOP technologies [13]. In this context, very different carbon-based nanostructured composites containing metallic nanoparticles have been recently applied with success in CWPO [14-16], their improved catalytic performance being ascribed to several synergistic effects that arise from the combination of the high catalytic activity of iron, or other metal species, with the easily tunable properties of carbon-based materials [13]. Furthermore, the magnetic properties of these catalysts may allow the implementation of in situ magnetic separation systems for catalyst recovery after reaction,

which would be an additional advantage to the process. Bearing this in mind, hybrid magnetic carbon composites may be considered the next step in the evolution of catalysts for CWPO [13]. In the light of these findings, a hybrid magnetic graphitic nanocomposite (MGNC) material was synthesised in the present work by hierarchical co-assembly of magnetic nanoparticles and carbon precursors, followed by thermal annealing. After a detailed characterization, the performance of MGNC in the CWPO of refractory organic pollutants was evaluated using 4-nitrophenol (4-NP) as model pollutant, in a very wide concentration range ($200 \text{ mg L}^{-1} - 5 \text{ g L}^{-1}$). In order to optimize the efficiency of catalyst usage, the MGNC catalyst dosage was kept very low when compared to the pollutant concentration, with a fixed pollutant/catalyst mass ratio as high as 10.

2. Materials and methods

2.1. Magnetite nanoparticles

Magnetite (Fe_3O_4) was synthesised by co-precipitation of Fe^{2+} and Fe^{3+} in basic solution, at $30 \text{ }^\circ\text{C}$ and under N_2 atmosphere, adapting a procedure described elsewhere [17]. For that purpose, 13.44 mmol of iron (II) chloride tetrahydrate and 26.88 mmol of iron (III) chloride hexahydrate were dissolved in 250 mL of distilled water and transferred into a 500 mL glass reactor, equipped with a condenser and immersed in an oil bath with controlled temperature. When the desired temperature was reached, the mixture was deaerated during 10 min with N_2 under vigorous stirring, and further kept under inert atmosphere. At this point, 10 mL of ammonium hydroxide solution ($25 \text{ wt.}\%$) were quickly added, a black precipitate being instantly obtained. Afterwards, possible residues of the precursors were washed-out with distilled water, the sample being then dried in an oven at $60 \text{ }^\circ\text{C}$ for 24 h , resulting in the Fe_3O_4 material.

2.2. Hybrid magnetic graphitic nanocomposites

The magnetic graphitic nanocomposite (MGNC) material was prepared by hierarchical co-assembly of Fe₃O₄ nanoparticles and carbon precursors, followed by thermal annealing, adapting the procedure described elsewhere [18]. For that purpose, 5 g of copolymer pluronic F127 were dissolved in 50 mL of H₂O, in a round bottom 500 mL glass reactor equipped with a condenser and immersed in an oil bath with temperature control. Then, 5 mL of Fe₃O₄ suspension (17 mg mL⁻¹, previously obtained by dispersion of Fe₃O₄ in H₂O in an ultrasonic bath) were added, the resulting solution being stirred during 2 h at 66 °C for homogenization. After that, ≈ 60 mL of a phenol/formaldehyde resol solution were added, the resulting mixture being kept under stirring (400 rpm) at 66 °C for 72 h and then at 70 °C for an additional 24 h. The phenol/formaldehyde resol solution was prepared by dissolution of 2.0 g of phenol in 7.0 mL of formaldehyde 37 wt.% solution, to which 50.0 mL of NaOH 0.1 mol L⁻¹ were added, the solution being then kept under stirring at 70 °C for 30 min.

The recovered solids were washed with distilled water in order to promote the wash-out of some possible residues of the precursors and then dried overnight in an oven at 60 °C. Afterwards the sample was thermally annealed under a N₂ flow (100 cm³ min⁻¹) at 120 °C, 400 °C and 600 °C during 60 min at each temperature and then at 800 °C for 240 min, defining a heating ramp of 2 °C min⁻¹. Finally, the sample was washed with 1 L of distilled water at 50 °C under vacuum filtration, and then with 1 L of HCl solution (pH = 3), also at 50 °C under vacuum filtration, being afterwards dried overnight in an oven at 60 °C, resulting in the MGNC material.

2.3. Characterization techniques

X-ray diffraction (XRD) analysis was performed in a PANalytical X'Pert MPD equipped with a X'Celerator detector and secondary monochromator

(Cu K α λ = 0.154 nm; data recorded at a 0.017 $^\circ$ step size). Highscore Plus and PowderCell software's were used to identify the crystallographic phases present and to calculate the crystallite sizes from Rietveld refinement of the XRD diffraction patterns. Transmission electron microscopy (TEM) was performed in a LEO 906E instrument operating at 120 kV, equipped with a 4 Mpixel 28 \times 28 mm CCD camera from TRS. 110 counts were performed for the determination of Fe₃O₄ particle size; 70 counts were performed for the determination of the metal core size of the MGNC catalyst. Textural characterization was performed in a Quantachrome NOVA 4200e adsorption analyser. Thermogravimetric analysis (TGA) was performed using a Netzsch STA 409 PC equipment under oxidative atmosphere. The pH of point of zero charge (pH_{PZC}) was determined by pH drift tests [19].

2.4. Catalytic wet peroxide oxidation experiments

Batch CWPO experiments were performed in a well-stirred (600 rpm) glass reactor equipped with a condenser, a temperature measurement thermocouple, a pH measurement electrode and a sample collection port. The reactor was loaded with 4-NP aqueous solutions (in the range 200 mg L⁻¹ – 5.0 g L⁻¹) and heated by immersion in an oil bath at controlled temperature. Upon stabilization at 80 $^\circ$ C, the solution pH was adjusted (in the range pH 3 – 9) by means of H₂SO₄ and NaOH solutions, and the experiments were allowed to proceed freely, without further conditioning of pH. A calculated volume of H₂O₂ (30% w/v) was injected into the system, in order to reach the stoichiometric amount of H₂O₂ needed to completely mineralise 4-NP (in the range 712 mg L⁻¹ – 17.8 g L⁻¹). The catalyst was added after complete homogenization of the resulting solution, that moment being considered as $t_0 = 0$ min. Pure adsorption runs were also performed in order to discriminate between adsorption and catalytic components of 4-NP removal by CWPO, but, in this case, the amount of H₂O₂ was replaced by distilled water. All the

experiments were performed considering the mass ratio $[4\text{-NP}]_0/[\text{Fe}_3\text{O}_4] = 36.6$, corresponding to a mass ratio $[4\text{-NP}]_0/[\text{MGNC}] = 10$ (27.3 wt.% of Fe_3O_4 in MGNC, as determined by TGA). Blank experiments, without any catalyst, were also carried out to assess possible non-catalytic oxidation promoted by H_2O_2 . In order to show the predominant role of heterogeneous catalysis promoted by MGNC, a leaching test was performed as proposed by Sheldon et al. [20], namely removing the MGNC catalyst after 30 min of reaction (ca. 37.5% 4-NP removal) at the reaction temperature (80 °C), and allowing the reaction solution to progress further.

The regeneration of the MGNC catalyst was performed using a simple H_2O_2 soaking technique, adapting the procedure described in reference [21]. For that purpose, the MGNC catalyst recovered from the first CWPO run performed with $[4\text{-NP}]_0 = 5 \text{ g L}^{-1}$ was contacted with H_2O_2 during 8 h under the same operation conditions used in the CWPO experiments, but in the absence of 4-NP (i.e., $T = 80 \text{ °C}$, $\text{pH} = 3$, $[\text{MGNC}] = 0.5 \text{ g L}^{-1}$ and $[\text{H}_2\text{O}_2]_0 = 17.8 \text{ g L}^{-1}$). The MGNC catalyst after regeneration was washed and dried at 60 °C overnight, and then reused in another CWPO run with a fresh 4-NP solution.

2.5. Analytical methods

4-NP and possible by-products of its oxidation were determined by high performance liquid chromatography, while the concentration of H_2O_2 was followed by a colorimetric method, as previously described [22]. Dissolved Fe content was determined by a colorimetric method with 1,10-phenantroline, according to ISO 6332 and measuring the absorbance at 510 nm [23]. Total organic carbon (TOC) was determined using a Shimadzu TOC-L CSN analyser.

3. Results and discussion

3.1. Textural and surface chemical characterization

Fe_3O_4 and MGNC were characterized by XRD and TEM, the corresponding results being given in Figure 1 and Figure 2, respectively. As observed from Figure 1, Fe_3O_4 exhibits the typical diffraction pattern of magnetite, with a lattice parameter $a = 8.357 \text{ \AA}$ and a crystallite size of $16.6 \pm 0.2 \text{ nm}$, which is near the average particle size of $12.5 \pm 3.6 \text{ nm}$ determined from TEM (cf. Figure 2e). Graphite, maghemite ($a = 8.379 \text{ \AA}$), iron ($a = 2.868 \text{ \AA}$) and traces of hematite (proto) were identified in the diffraction pattern of MGNC (cf. Figure 1), in addition to magnetite ($a = 8.343 \text{ \AA}$). This result suggests that Fe_3O_4 nanoparticles were successfully encapsulated within a graphitic structure during the synthesis of MGNC, although with some changes in the magnetite phase. This fact is also supported by the TEM micrographs depicted in Figure 2b-d, in which the core-shell structure of MGNC is unequivocally demonstrated. In particular, the TEM micrograph obtained in dark field mode (cf. Figure 2c) confirms the existence of crystalline cores inside the carbon shells. The average size of the magnetic core of MGNC, $109 \pm 35 \text{ nm}$, as determined from TEM measurements (cf. Figure 2f), suggests that the cores are mainly composed by agglomerates of magnetic nanoparticles (with crystallite sizes in the range $23 - 165 \text{ nm}$, depending on the phase, as determined by XRD analysis). These observations are in accordance with the hierarchical co-assembly mechanism of the MGNC synthesis, as detailed elsewhere [18]. During this procedure, Fe_3O_4 nanocrystals grow and spontaneously co-assemble by partially replacing F127/resol micelles; at the same time, carbon-carbon bonds are formed with the polymerization of resols and, upon thermal annealing, the copolymer F127 is eliminated, graphitic carbon frameworks being obtained with the participation of Fe_3O_4 as graphitization catalyst [18].

FIGURE 1

FIGURE 2

The texture and surface chemistry of MGNC were further characterized by TGA analysis, N₂ adsorption-desorption isotherms and pH_{PZC}. The TGA analysis of MGNC (cf. Figure 3a) reveals 27.3 wt.% of ashes, corresponding to the mass fraction of Fe₃O₄ encapsulated in MGNC. It was also found that MGNC is stable up to 400 °C under oxidizing atmosphere. The N₂ adsorption-desorption isotherms at -196 °C of MGNC (cf. Figure 3b) show a hysteresis loop of type H4 in accordance with IUPAC classification, typical of micro-mesoporous carbon materials [24]. MGNC possesses a specific surface area (S_{BET}) of 330 m² g⁻¹, a non-microporous specific surface area (S_{meso}) of 170 m² g⁻¹, a total pore volume (V_{total}) of 0.31 cm³ g⁻¹ and a micropore volume (V_{micro}) of 0.07 cm³ g⁻¹. The micro-mesoporous character of MGNC is particularly reflected by the ratio V_{mic}/V_{total} = 0.24, as well as an average pore diameter of 3.7 nm. Regarding the surface chemistry, the pH_{PZC} of MGNC (7.1) reveals that most of the acidic and basic functionalities were removed during the thermal annealing.

3.2. Catalytic wet peroxide oxidation experiments

The performance of MGNC in the CWPO of 4-NP solutions was initially evaluated against that of bare Fe₃O₄, in experiments performed with 200 mg L⁻¹ 4-NP solutions, and always maintaining a 4-NP/ Fe₃O₄ mass ratio of 36.6. As observed in Figure 4a, the 4-NP removal obtained after 2 h in the non-catalytic H₂O₂ experiment is not significant (representing a TOC removal of 0.6% only), while a fast removal of 4-NP is achieved in the presence of the Fe₂O₃ catalyst. In addition, the catalytic activity is enhanced when the Fe₃O₄ magnetic material is encapsulated within a carbon shell in the MGNC catalyst. To the best of our knowledge, this effect was first reported with hybrid magnetic carbon composites by Hu et al. in 2011 [14], but other authors have reached the same conclusion in the meantime [13]. This behaviour may be explained by the presence of the carbon

phase, which increases the adsorptive interactions between the surface of the catalyst and the pollutant molecules, attracting higher amounts of pollutant molecules to the vicinity of the active sites where highly oxidizing HO[•] radicals are generated, thus inhibiting non-efficient parasitic reactions involving H₂O₂ and HO[•] [13]. Specifically, it was found that the adsorption of 4-NP obtained with MGNC amounts to 100.8 mg g⁻¹ after 2 h, while there is no adsorption on Fe₃O₄ under the same conditions (data not shown). In addition, the electron transfer features of carbon-based materials, as well as their potential intrinsic catalytic activity in CWPO, may also contribute to enhance the catalytic decomposition of H₂O₂ and the subsequent oxidation of 4-NP molecules [13]. Nevertheless, by comparing the leaching of Fe species at the end of the CWPO experiments performed with Fe₃O₄ (0.98 mg L⁻¹) and MGNC (0.27 mg L⁻¹), the main synergistic effect arising from the inclusion of Fe₃O₄ nanoparticles into a carbon structure during the synthesis of MGNC is unequivocally highlighted (as inferred from the ca. 4-fold decrease of Fe leaching observed). These observations allow to conclude that the lower leaching of Fe species obtained with MGNC is due to the confinement effect caused by the carbon shell, as recently found for other hybrid magnetic carbon composites applied in CWPO [13].

Complementary data for MGNC are shown in Figure 4b. Regarding the mineralization of 4-NP, ca. 29% of TOC removal is achieved upon application of the MGNC catalyst – a value that increases up to ca. 60% when the CWPO experiment is allowed to proceed during 8 h. At the same time, the consumption of H₂O₂ amounts to ca. 45% after 2 h and to ca. 60% after 8 h of reaction, which represents efficiencies of TOC removal per unit of H₂O₂ decomposed ($\eta_{\text{H}_2\text{O}_2}$) in the range 64 – 100%. In addition, the removal of 4-NP obtained in the pure adsorption run performed with MGNC is negligible, suggesting the wide prevalence of the catalytic component in the 4-NP removal by CWPO. The predominant role of heterogeneous CWPO promoted by MGNC is also well evidenced in

Figure 4b, through the leaching test performed as described in the experimental Section. Specifically, when the MGNC catalyst is removed after 30 min of reaction (ca. 37.5% 4-NP removal), the reaction solution reveals negligible activity in the CWPO of 4-NP, when considering both 4-NP and TOC removals. All these observations, together with the magnetic properties of MGNC (cf. inset of Figure 4b) and the very high pollutant mass removal of $5000 \text{ mg g}^{-1} \text{ h}^{-1}$ obtained – which is unprecedented in CWPO processes with carbon-based [13] and magnetite-based catalysts [25], open a window of opportunity, not only for the application of MGNC in CWPO, but also for the development of in-situ magnetic separation systems. Therefore, MGNC was object of additional studies.

FIGURE 3

The individual effect of the solution pH on the performance of MGNC in CWPO was evaluated, as shown in Figure 4c. As observed, when CWPO is carried out without adjustment of the natural pH of the 4-NP solution (i.e., at pH = 6), MGNC reveals some catalytic activity, with ca. 42% of the initial pollutant being removed. Although the complete abatement of 4-NP is not achieved under these conditions, the pollutant mass removal obtained ($2090 \text{ mg g}^{-1} \text{ h}^{-1}$) is still higher than that reported in the literature for carbon-based [13] and magnetite-based catalysts [25]. Nevertheless, MGNC loses most of its catalytic activity when the initial pH is increased to 9, with only ca. 11% of the parent pollutant being removed.

FIGURE 4

3.2.1. Process intensification

In order to assess the possibility of MGNC to act as a high performance catalyst in CWPO processes under intensified conditions, which may be potentially more attractive for industrial applications (i.e., to treat wastewaters with higher pollutant concentrations), the 4-NP concentration was increased 5-fold, to 1 g L^{-1} , employing the same 4-NP/ Fe_3O_4

mass ratio of 36.6. Likewise, the H₂O₂ dosage was kept at the stoichiometric amount needed to completely mineralise 4-NP. As observed in Figure 5a, complete 4-NP removal is obtained after 4 h in experiments performed under these conditions, corresponding to a pollutant mass removal of 2500 mg g⁻¹ h⁻¹. Afterwards, the initial 4-NP concentration was again increased 5-fold, reaching a significantly high concentration of 5 g L⁻¹, while keeping the 4-NP/ Fe₃O₄ mass ratio and feeding H₂O₂ at the stoichiometric amount for 4-NP mineralisation. As observed in Figure 5a, complete 4-NP removal is also achieved even under these operating conditions, provided that the CWPO reaction is allowed to proceed during 8 h. In this case, the pollutant mass removal obtained amounts to 1250 mg g⁻¹ h⁻¹, which is much higher than that reported for carbon-based catalysts [13] and similar to the best results reported for magnetite-based catalysts operating with ca. 8-fold lower pollutant concentrations [25].

It is noteworthy that after the initial adjustment, the experiments were allowed to proceed without further conditioning of pH. Therefore, the initial 4-NP concentration is expected to strongly influence the pH of the treated water, particularly when the aromatic ring of the 4-NP molecule is open and carboxylic acids are formed (cf. Section 3.2.3 for details). Bearing this in mind, the pH of the treated water was measured at the end of the CWPO experiments. It was observed that the final pH dropped from 3 to 2.79, 2.45 and 1.79, when the initial 4-NP concentration was 200 mg L⁻¹, 1 g L⁻¹ and 5 g L⁻¹, respectively. Nevertheless, even with the most pronounced decrease of the solution pH, the Fe leached to the treated water during the experiment performed with 5 g L⁻¹ 4-NP solutions was 1.8 mg L⁻¹ – a value still below the limits allowed by common EU directives for treated water to be discharged into natural receiving water bodies (2 mg L⁻¹).

In order to evaluate the efficiency of H₂O₂ consumption when MGNC is applied in the CWPO of 4-NP solutions in the concentration range studied, the TOC conversion (X_{TOC})

was plotted against the H_2O_2 conversion ($X_{\text{H}_2\text{O}_2}$) obtained in each experiment (cf. Figure 5b). The high $\eta_{\text{H}_2\text{O}_2}$ previously observed when $[\text{4-NP}]_0 = 200 \text{ mg L}^{-1}$ is improved when higher pollutant concentrations are considered. Specifically, the values of X_{TOC} are similar to those of $X_{\text{H}_2\text{O}_2}$, suggesting $\eta_{\text{H}_2\text{O}_2}$ of ca. 100%. Therefore, it is possible to conclude that, in addition to the highly efficient usage of the catalyst, the H_2O_2 employed in the CWPO process with MGNC is also consumed with rather high efficiency across the wide 4-NP concentration range studied.

FIGURE 5

3.2.2. Reusability cycles

In order to assess the stability of MGNC – a basic requirement for industrial scale applications – this catalyst was tested in two series of consecutive CWPO runs, performed with 200 mg L^{-1} and 5 g L^{-1} 4-NP solutions. For that purpose, after each run, the catalyst was filtered, washed and dried at $60 \text{ }^\circ\text{C}$ overnight, and then reused in CWPO with a fresh 4-NP solution. The 4-NP and TOC removals obtained in these two series of experiments are given in Figure 6. As observed, 4-NP removal slightly decreases from 100%, in the first run, to 96%, in the fourth run, in the experiments performed with 200 mg L^{-1} 4-NP solutions. As previously shown in the CWPO of phenol over microporous activated carbon catalysts [26], as well as in the CWPO of 2-nitrophenol over glycerol-based carbon catalysts [27], the decrease of the MGNC catalytic activity may be partially caused by 4-NP reaction by-products adsorbed or deposited on the carbon surface, which limit the accessibility to the active sites. Nevertheless, the pollutant mass removal obtained in the fourth CWPO cycle performed with MGNC ($4808 \text{ mg g}^{-1} \text{ h}^{-1}$) is still far above the values reported in CWPO processes performed with carbon-based [13] and magnetite-based catalysts [25]. Under these conditions, the TOC removal obtained after 2 h of reaction with MGNC is not particularly affected by the successive reuse of the catalyst..

Similar results, though with more pronounced effects, were observed in the reusability cycles performed with 5 g L^{-1} 4-NP solutions. In this case, the higher entropy of the system promotes harsher conditions, with higher concentration of by-products of 4-NP oxidation, which may result in the higher decrease of the catalytic performance of MGNC upon successive reuse cycles. Nevertheless, the pollutant mass removal obtained in the third CWPO cycle performed under these conditions ($551 \text{ mg g}^{-1} \text{ h}^{-1}$) is still quite good when compared to other catalysts [13, 25].

In order to demonstrate the influence of by-products deposition, a simple regeneration procedure of the MGNC catalyst recovered from the first CWPO run was performed by H_2O_2 soaking, as detailed in Section 2.4. In this way, the oxidation of the by-products adsorbed at the surface of the MGNC catalyst is promoted. As observed in Figure 6, the catalytic activity of MGNC is partially restored through this simple regeneration approach. This observation confirms that the decrease of the MGNC performance in successive CWPO runs is in part explained by the adsorption or deposition of by-products of 4-NP oxidation on the carbon surface of MGNC.

In addition, MGNC can be considered fairly stable against the leaching of Fe species to the treated water throughout the wide 4-NP concentration range studied. For instance, the Fe leached during the CWPO cycles performed with 200 mg L^{-1} 4-NP solutions remains nearly constant, going from only 0.27 mg L^{-1} , in the first cycle, to 0.33 mg L^{-1} in the fourth cycle. Even in the experiments performed with intensified conditions, considering 5 g L^{-1} 4-NP solutions, the Fe leached is always kept below the limits allowed by EU directives for treated water to be discharged into natural receiving water bodies (1.8 mg L^{-1} in the first cycle, 1.3 mg L^{-1} in the second cycle and only 0.3 mg L^{-1} in the third cycle performed with MGNC; while the leaching of Fe species during the experiment with the MGNC regenerated after the first CWPO cycle was 1.2 mg L^{-1}). The

negligible Fe leaching levels observed in the third cycles performed, allow concluding about the predominant role of heterogeneous catalysis over that possibly promoted by homogeneous Fe species leached into the solution. This conclusion is further supported on the results shown in Figure 4a, in which it was found that the catalytic activity of MGNC is superior to that of bare Fe₃O₄, in spite of the much higher Fe leaching resulting from the application of Fe₃O₄ (0.98 mg L⁻¹, against 0.27 mg L⁻¹ when MGNC is applied), as well as on the results obtained in the leaching test performed (cf. Figure 4b).

FIGURE 6

3.2.3. Oxidation mechanism

In order to demonstrate the oxidation/mineralization mechanism during the CWPO of 4-NP in the presence of MGNC, the evolution of possible aromatic (a) and non-aromatic (b) by-products was assessed in the experiment performed with the highest 4-NP concentration (cf. Figure 7). As the reaction mechanism of HO[•] radicals with aromatic compounds is known to proceed mainly through electrophilic addition to the aromatic ring, the presence of the phenolic –OH group together with the –NO₂ group, in the case of 4-NP, is favourable to an electrophilic attack at the *ortho* position in respect to the –OH group, leading to the formation of 4-nitrocatechol [22]. As observed in Figure 7a, 4-nitrocatechol is the main aromatic by-product of the 4-NP mineralization by CWPO in the presence of MGNC. However, the presence of 4-nitrocatechol is rather low after 8 h of reaction. Hydroquinone, 1,4-benzoquinone and catechol were also observed, which is in accordance with the mechanism previously proposed for the CWPO of 4-NP [22]. Further attack of HO[•] radicals on the aromatic intermediate compounds leads to the opening of the aromatic ring, and thus to the formation of a series of low molecular weight carboxylic acids (cf. Figure 7b) [22][21].

FIGURE 7

4. Conclusions

The main conclusion withdrawn from this work is that the inclusion of Fe₃O₄ nanoparticles in a graphitic structure during the synthesis of MGNC (i) enhances the catalytic activity in the CWPO of 4-NP when compared to Fe₃O₄, due to increased adsorptive interactions between the surface of the catalyst and the pollutant molecules, while (ii) strongly limiting the leaching of Fe species from Fe₃O₄ to the treated water, due to the confinement effect caused by the carbon shell. As a result of these effects, unprecedented pollutant mass removals were obtained.

Although partial deactivation occurs through successive reusability cycles, the performance of the MGNC catalyst is still high at the end of the fourth cycle, with only a ca. 4% decrease of pollutant removal being observed when 200 mg L⁻¹ 4-NP solutions are considered. The harsher conditions promoted by 5 g L⁻¹ 4-NP solutions lead to a higher deactivation of the MGNC catalyst. Nevertheless, the pollutant mass removal obtained at the end of the third cycle under these conditions is still high.

Acknowledgments

This work was financially supported by: Project POCI-01-0145-FEDER-006984 – Associated Laboratory LSRE/LCM funded by FEDER funds through COMPETE2020 - Programa Operacional Competitividade e Internacionalização (POCI) – and by national funds through FCT - Fundação para a Ciência e a Tecnologia. R.S. Ribeiro acknowledges the FCT individual Ph.D. grant SFRH/BD/94177/2013, with financing from FCT and the European Social Fund (through POPH and QREN). A.M.T. Silva acknowledges the FCT Investigator 2013 Programme (IF/01501/2013), with financing from the European Social Fund and the Human Potential Operational Programme.

References

- [1] O. Abdelwahab, N.K. Amin, E.S.Z. El-Ashtoukhy, *J. Hazard. Mater.* 163 (2009) 711-716.
- [2] S. Ahmed, M.G. Rasul, W.N. Martens, R. Brown, M.A. Hashib, *Desalination* 261 (2010) 3-18.
- [3] M. Diao, N. Ouédraogo, L. Baba-Moussa, P. Savadogo, A. N'Guessan, I.N. Bassolé, M. Dicko, *Biodegradation* 22 (2011) 389-396.
- [4] E.-S.Z. El-Ashtoukhy, Y.A. El-Taweel, O. Abdelwahab, E.M. Nassef, *Int. J. Electrochem. Sci.* 8 (2013) 1534 - 1550.
- [5] Y. Kurata, Y. Ono, Y. Ono, *J. Mater. Cycles Waste Manag.* 10 (2008) 144-152.
- [6] X. Peng, Y. Yu, C. Tang, J. Tan, Q. Huang, Z. Wang, *Sci. Total Environ.* 397 (2008) 158-166.
- [7] R. Andreozzi, V. Caprio, A. Insola, R. Marotta, *Catal. Today* 53 (1999) 51-59.
- [8] P.R. Gogate, A.B. Pandit, *Adv. Environ. Res.* 8 (2004) 501-551.
- [9] S. Navalon, M. Alvaro, H. Garcia, *Appl. Catal., B* 99 (2010) 1-26.
- [10] C.W. Jones, *Applications of hydrogen peroxide and derivatives*, The Royal Society of Chemistry, Cambridge, UK, 1999.
- [11] J.J. Pignatello, E. Oliveros, A. MacKay, *Crit. Rev. Environ. Sci. Technol.* 36 (2006) 1-84.
- [12] M. Pera-Titus, V. García-Molina, M.A. Baños, J. Giménez, S. Esplugas, *Appl. Catal., B* 47 (2004) 219-256.
- [13] R.S. Ribeiro, A.M.T. Silva, J.L. Figueiredo, J.L. Faria, H.T. Gomes, *Appl. Catal., B* 187 (2016) 428-460.
- [14] X. Hu, B. Liu, Y. Deng, H. Chen, S. Luo, C. Sun, P. Yang, S. Yang, *Appl. Catal., B* 107 (2011) 274-283.

- [15] W. Liu, J. Qian, K. Wang, H. Xu, D. Jiang, Q. Liu, X. Yang, H. Li, J. Inorg. Organomet. Polym. Mater. 23 (2013) 907-916.
- [16] X. Zhang, M. He, J.-H. Liu, R. Liao, L. Zhao, J. Xie, R. Wang, S.-T. Yang, H. Wang, Y. Liu, Chin. Sci. Bull. 59 (2014) 3406-3412.
- [17] K. Rusevova, F.-D. Kopinke, A. Georgi, J. Hazard. Mater. 241–242 (2012) 433-440.
- [18] R. Liu, L. Wan, S. Liu, Y. Yu, S. Li, D. Wu, J. Colloid Interface Sci. 414 (2014) 59-65.
- [19] H.T. Gomes, S.M. Miranda, M.J. Sampaio, A.M.T. Silva, J.L. Faria, Catal. Today 151 (2010) 153-158.
- [20] R.A. Sheldon, M. Wallau, I.W.C.E. Arends, U. Schuchardt, Acc. Chem. Res. 31 (1998) 485-493.
- [21] L.-X. Hu, D.-D. Xu, L.-P. Zou, H. Yuan, X. Hu, Acta Phys. Chim. Sin. 31 (2015) 771-782.
- [22] R.S. Ribeiro, A.M.T. Silva, L.M. Pastrana-Martínez, J.L. Figueiredo, J.L. Faria, H.T. Gomes, Catal. Today 249 (2015) 204–212.
- [23] ISO 6332:1988, Water quality - Determination of iron - Spectrometric method using 1,10-phenanthroline, International Organization for Standardization, 1988.
- [24] M. Thommes, K. Kaneko, A.V. Neimark, J.P. Olivier, F. Rodriguez-Reinoso, J. Rouquerol, K.S.W. Sing, Pure Appl. Chem. 87 (2015) 1051-1069.
- [25] M. Munoz, Z.M. de Pedro, J.A. Casas, J.J. Rodriguez, Appl. Catal., B 176–177 (2015) 249-265.
- [26] C.M. Domínguez, P. Ocón, A. Quintanilla, J.A. Casas, J.J. Rodríguez, Appl. Catal., B 140–141 (2013) 663-670.
- [27] R.S. Ribeiro, A.M.T. Silva, M.T. Pinho, J.L. Figueiredo, J.L. Faria, H.T. Gomes, Catal. Today 240, Part A (2015) 61-66.

FIGURE CAPTIONS

Figure 1. XRD diffraction patterns of Fe_3O_4 and MGNC.

Figure 2. TEM micrographs of (a) Fe_3O_4 and (b-d) MGNC: (b and d) and (c) were obtained in bright field and dark field image modes, respectively. Histogram of particle size distribution: (e) Fe_3O_4 and (f) magnetic core of MGNC determined by TEM.

Figure 3. (a) Thermogravimetric analysis (TGA) of MGNC in air atmosphere; (b) N_2 adsorption-desorption isotherm at $-196\text{ }^\circ\text{C}$ of MGNC.

Figure 4. (a) Removal of 4-NP obtained as a function of time in CWPO runs performed with Fe_3O_4 , MGNC and in the absence of catalyst (non-catalytic). (b) 4-NP, TOC and H_2O_2 conversions as a function of time in the CWPO run performed with MGNC (Inset: magnetic separation of the MGNC catalyst in distilled water), as well as 4-NP and TOC removals obtained during the “leaching test” performed with MGNC (i.e. where the catalyst was removed from the solution after 30 min of reaction); 4-NP removals by adsorption are also shown for comparison. (c) Effect of the initial pH on the CWPO removal of 4-NP when using the MGNC catalyst. Experiments performed with $[\text{4-NP}]_0 = 200\text{ mg L}^{-1}$, $[\text{MGNC}] = 20\text{ mg L}^{-1}$, $[\text{Fe}_3\text{O}_4] = 5.5\text{ mg L}^{-1}$ (corresponding to 27.3 wt.% of MGNC), $T = 80\text{ }^\circ\text{C}$, $[\text{H}_2\text{O}_2]_0 = [\text{H}_2\text{O}_2]_{\text{Stoichiometric}} = 712\text{ mg L}^{-1}$ (in CWPO runs) and (a and b) $\text{pH} = 3$. Inset of (b): magnetic separation of MGNC in distilled water.

Figure 5. (a) Removal of 4-NP obtained as a function of time in CWPO runs performed with MGNC under different operative conditions and (b) corresponding TOC vs H_2O_2 conversions obtained after 2, 4 and 8 h, when considering $[\text{4-NP}]_0 = 200\text{ mg L}^{-1}$, 1 g L^{-1} and 5 g L^{-1} , respectively. Experiments performed with a mass ratio $[\text{4-NP}]_0/[\text{MGNC}] = 10$, $T = 80\text{ }^\circ\text{C}$, $\text{pH} = 3$ and $[\text{H}_2\text{O}_2]_0 = [\text{H}_2\text{O}_2]_{\text{Stoichiometric}}$.

Figure 6. 4-NP and TOC conversions obtained in a series of consecutive CWPO runs performed with MGNC under the experimental conditions of Figure 5. Data obtained

after 2 and 8 h of reaction, when considering $[4\text{-NP}]_0 = 200 \text{ mg L}^{-1}$ and 5 g L^{-1} , respectively. Results obtained with MGNC regenerated after the first CWPO run performed with $[4\text{-NP}]_0 = 5 \text{ g L}^{-1}$ are also given.

Figure 7. Evolution of aromatic (a) and non-aromatic (b) by-products of 4-NP oxidation, when using MGNC in the CWPO process developed with $[4\text{-NP}]_0 = 5 \text{ g L}^{-1}$, $[\text{MGNC}] = 0.5 \text{ g L}^{-1}$, $T = 80 \text{ }^\circ\text{C}$, $\text{pH} = 3$ and $[\text{H}_2\text{O}_2]_0 = [\text{H}_2\text{O}_2]_{\text{Stoichiometric}} = 17.8 \text{ g L}^{-1}$.

FIGURE 1

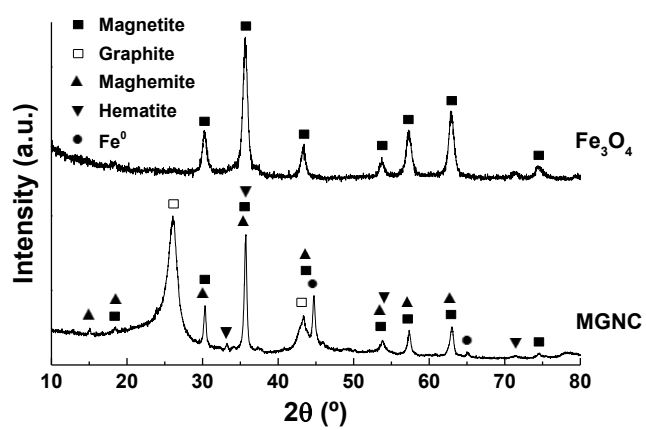


FIGURE 2

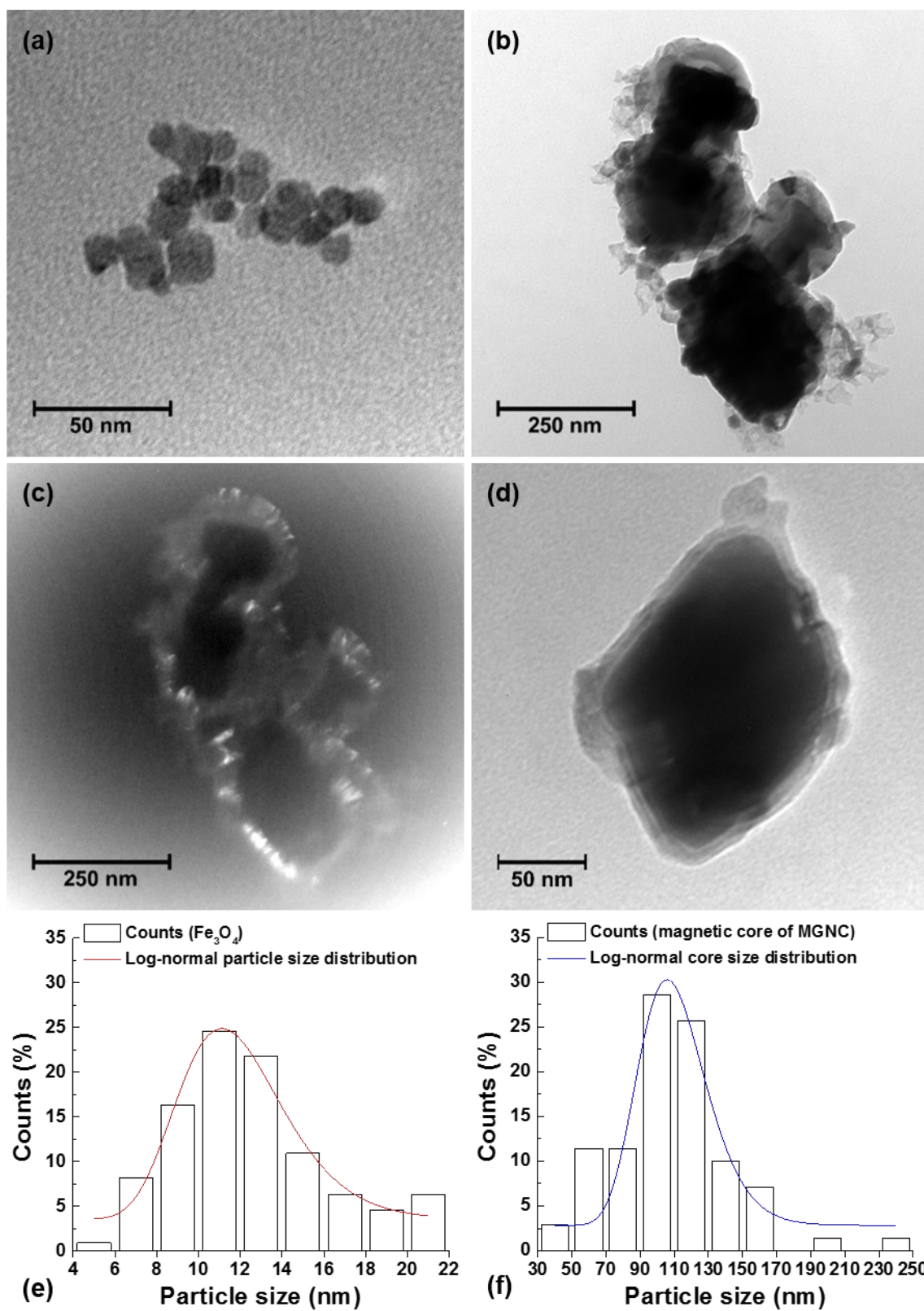


FIGURE 3

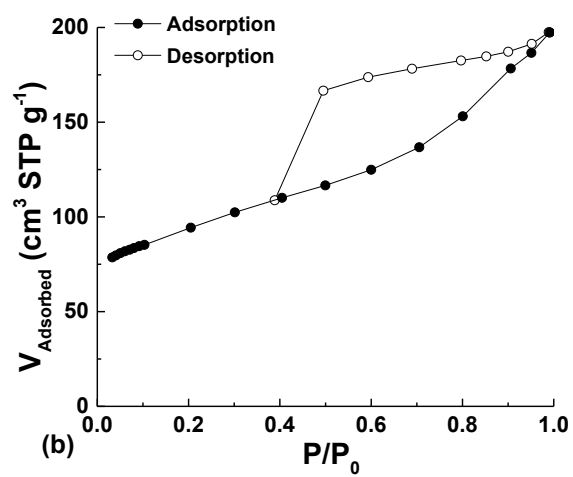
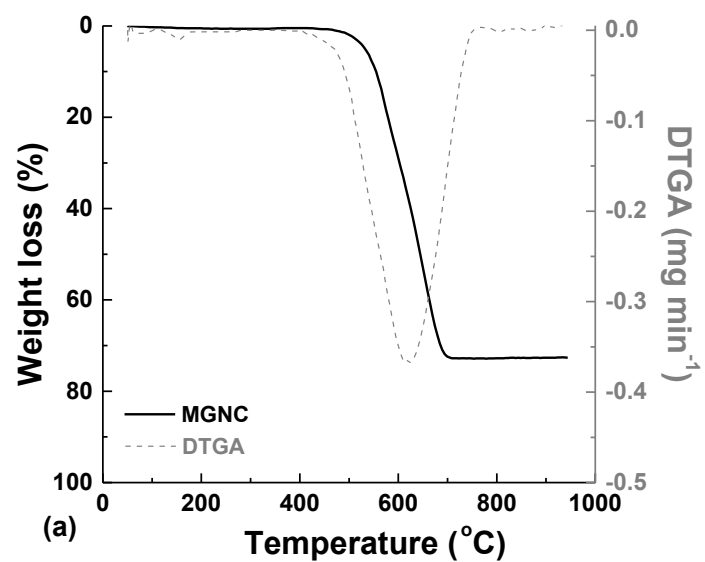


FIGURE 4

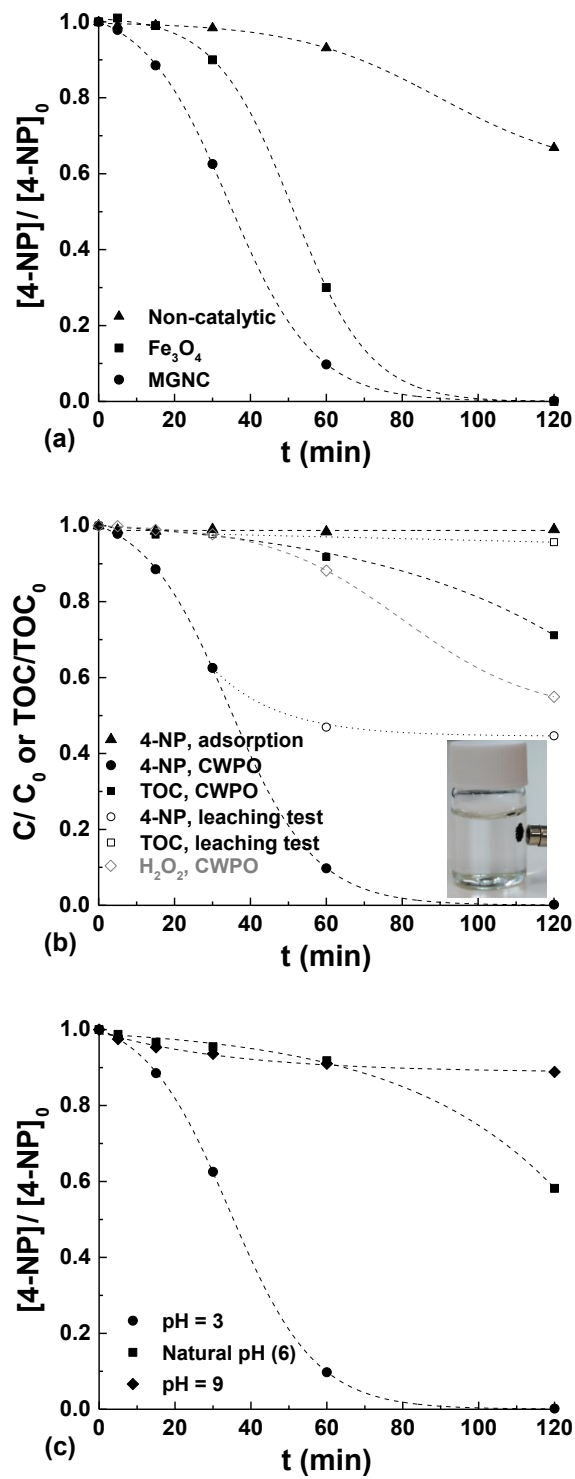


FIGURE 5

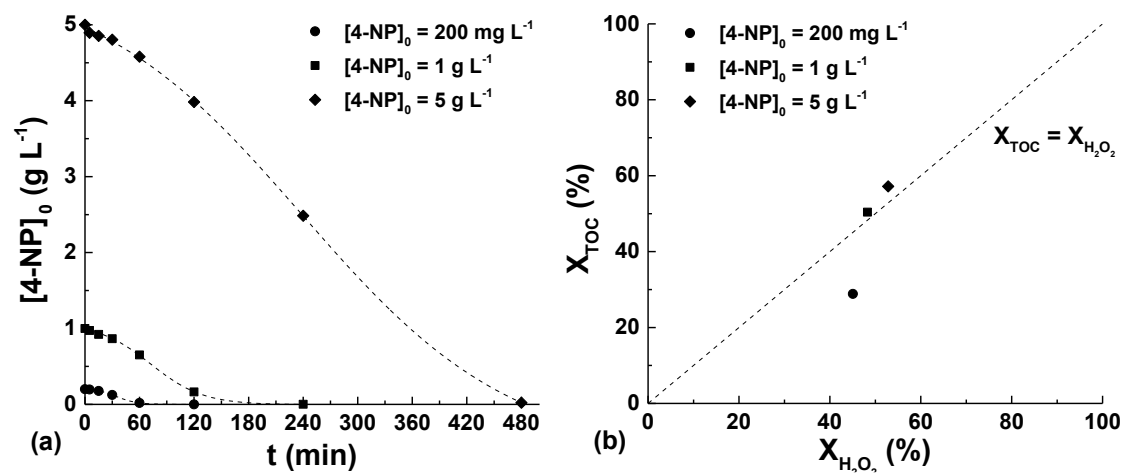


FIGURE 6

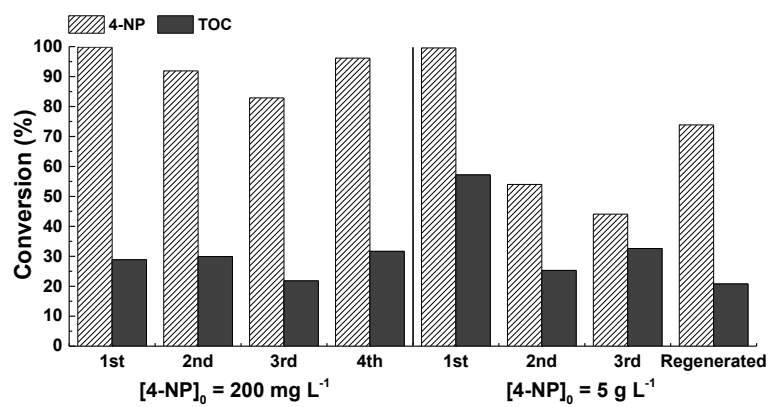


FIGURE 7

